

Quantum Gravity Corrections to the Scalar Quasi-Normal Modes in Near-Extremal Reissner-Nordström Black Holes

Zheng Jiang^{1,2,*}, Jun Nian^{1,3,†}, Caiying Shao^{2,‡}, Yu Tian^{1,2,§} and Hongbao Zhang^{4,5,¶}

¹*International Centre for Theoretical Physics Asia-Pacific,
University of Chinese Academy of Sciences, 100190 Beijing, China*

²*School of Physical Sciences, University of Chinese Academy of Sciences, 100049 Beijing, China*

³*Peng Huanwu Center for Fundamental Theory, Hefei, Anhui 230026, China*

⁴*School of Physics and Astronomy, Beijing Normal University, Beijing 100875, China*

⁵*Key Laboratory of Multiscale Spin Physics, Ministry of Education,
Beijing Normal University, Beijing 100875, China*

We investigate quantum corrections to scalar quasi-normal modes (QNMs) in the near-extremal Reissner–Nordström black hole background with quantum correction in the near-horizon $\text{AdS}_2 \times \text{S}^2$ region. By performing a dimensional reduction, we obtain an effective Jackiw–Teitelboim (JT) gravity theory, whose quantum fluctuations are captured by the Schwarzian action. Using path integral techniques, we derive the quantum-corrected scalar field equation, which modifies the effective potential governing the QNMs. These corrections are extended from the near-horizon region to the full spacetime via a matching procedure. We compute the corrected QNMs using both the third-order WKB method and the Prony method and find consistent results. Our analysis reveals that quantum corrections can lead to substantial shifts in the real parts of QNM frequencies, particularly for small-mass or near-extremal black holes, while the imaginary parts remain relatively stable. This suggests that quantum gravity effects may leave observable imprints on black hole perturbation spectra, which could be potentially relevant for primordial or microscopic black holes.

I. INTRODUCTION

Black holes should not be viewed as isolated systems in real physics problems [1]. Especially interesting in this regard is the linear perturbation theory. If the perturbation is performed, the late-time behavior should be a superposition of many exponentially-damped modes, whose complex frequencies ω are properties of the black hole, independent of the initial perturbation. These complex frequencies are then referred to as quasi-normal modes (QNMs) [2], which have attracted considerable interest.

For the linear perturbation theory in a black hole background, the master equation for the quasi-normal modes is the Schrödinger-like equation $\partial_x^2 \psi + (\omega^2 - V(x))\psi = 0$ [3], where x represents the tortoise coordinate, and $V(x)$ takes different forms depending on the fields and the black hole background.

Thermal fluctuations are suppressed in the low temperature regime, due to the Boltzmann factor $\exp(-1/k_B T)$. However, quantum fluctuations, which originate from the Heisenberg uncertainty principle and persist even at zero temperature, become dominant in the dynamical behavior of the system. Hence, in the near-extremal limit, the temperature is low and the quantum fluctuations become important. In our paper, we investigate the quantum corrections to the scalar quasi-normal modes due to the quantum fluctuations of the near-extremal RN black

holes.

For extremal and near-extremal RN black holes, the near-horizon region is $\text{AdS}_2 \times \text{S}^2$. Upon dimensional reduction to the near-horizon AdS_2 throat region, we obtain an AdS_2 Jackiw-Teitelboim gravity [4, 5]. According to the AdS/CFT correspondence, the dual theory of the two-dimensional Jackiw-Teitelboim (JT) gravity is the one-dimensional Schwarzian theory.

Over the last decade, the AdS_2 -JT gravity/Schwarzian theory duality has garnered significant research interest, and considerable progress has been made. First, the backreaction of the dilaton gravity in AdS_2 was considered in [6]. For the AdS_2 -JT theory, the bulk action is a dilaton field coupled to the Einstein-Hilbert action. As discussed in [7], the IR theory of gravity can be determined by the boundary cutoff. If we fix the proper length of the cutoff curve, we will see that the quantum fluctuations of the AdS_2 metric can be viewed as the reparametrization of the cutoff curve. Integrating out the bulk part of the AdS_2 -JT gravity, the boundary extrinsic derivative is shown to be proportional to the Schwarzian derivative with respect to the reparametrization modes, which are consequently named the Schwarzian modes.

We can expand the fluctuating AdS_2 metric and the physical quantities associated with it in terms of the Schwarzian modes. By introducing an auxiliary field, [8] shows that the path integral of the Schwarzian theory is one-loop exact. The correlators of the Schwarzian modes at the one-loop level are obtained in [9]. Hence, using the Schwarzian action, we obtain the quantum gravity corrections of physical quantities if they are minimally coupled to the AdS_2 -JT gravity.

Some previous work along this line includes the quantum correction to geometric physical quantities [10],

* jiangzheng22@mails.ucas.ac.cn

† nianjun@ucas.ac.cn

‡ shaocaiying@ucas.ac.cn

§ ytian@ucas.ac.cn

¶ hongbaozhang@bnu.edu.cn

black hole evaporation in 2d JT gravity [11], and defects in 2d JT gravity [12], among others. While most of these papers treat the path integral of 2d JT gravity or 1d Schwarzian theory directly, in this paper, we evaluate the correlators perturbatively.

More specifically, to discuss the physical quantities in the near-extremal RN black hole background, we first need to perform a dimensional reduction. As discussed in [13], the near-horizon region of a near-extremal RN black hole can yield AdS₂-JT gravity. The Euclidean path integral of such an effective theory can be computed exactly by first integrating out the gauge degrees of freedom [14], which also applies for the neutral scalar fields considered in this paper, and then by analyzing the Schwarzian modes. Hence, calculating quantum corrections in the near-horizon region involves finding the Schwinger-Dyson equation for the Schwarzian modes. For the far region, the quantum fluctuation should be small, which makes the far region essentially classical. However, there is an overlapping region between the near-horizon and far regions, which can carry quantum corrections from the near-horizon region to the far region. From this viewpoint, we can extend the Schwinger-Dyson equation from the near-horizon region to the whole RN spacetime. Similar ideas have been applied to compute the quantum-corrected greybody factor of the Hawking radiation for various near-extremal black holes [15–17]. In contrast to these works, we will study the quantum-corrected matter field equations in this paper.

The plan of this paper is as follows. In Sec. II, we will discuss how to introduce quantum corrections to the physical quantities in the near-extremal RN black hole background. In Sec. III, we will show how to calculate the scalar quasi-normal modes. In Sec. IV, we will list the results of quantum corrections to the scalar quasi-normal modes. Some discussions and outlooks are presented in Sec. V.

II. QUANTUM CORRECTION TO AdS₂ SPACETIME AND RN BLACK HOLE

A. From Reissner-Nordström Black Hole to AdS₂ Spacetime

For the RN black hole, the metric is given by

$$ds^2 = f(r)dt^2 + \frac{dr^2}{f(r)} + r^2 d\theta^2 + r^2 \sin^2 \theta d\varphi^2, \quad (1)$$

where the function $f(r)$ is given by the mass M and the charge Q of the black hole, as

$$f(r) = 1 - \frac{2M}{r} + \frac{Q^2}{r^2}. \quad (2)$$

The radius of its horizon is given by

$$f(r) = 0, \quad (3)$$

hence, there are two horizons for the RN black hole,

$$r_{\pm} = M \pm \sqrt{M^2 - Q^2}. \quad (4)$$

The Hawking temperature of an RN black hole is given as

$$T = \frac{r_+ - r_-}{8\pi M r_+} = \frac{\sqrt{M^2 - Q^2}}{4\pi M(M + \sqrt{M^2 - Q^2})}. \quad (5)$$

When the black hole is extremal, $M = |Q|$, the two horizons coincide

$$r_+ = r_- = r_h = M. \quad (6)$$

While for the near-extremal black hole, two horizons come very close,

$$r_{\pm} = r_h \pm \delta, \quad \delta = \sqrt{M^2 - Q^2} \ll M. \quad (7)$$

Considering the near-horizon region of an extremal RN black hole, i.e., $\frac{r-r_h}{r_h} \ll 1$, the metric can be written as

$$ds^2 = -\frac{r'^2 - \delta^2}{r_h^2} dt^2 + \frac{r_h^2}{r'^2 - \delta^2} dr^2 + r_h^2 d\Omega_2^2, \quad (8)$$

where $r' = r - r_h$ and $d\Omega_2^2 = d\theta^2 + \sin^2 \theta d\varphi^2$. Performing the coordinate transformation, $r' = \delta \coth \delta z'$, $t' = t/r_h^2$, then the near-horizon region becomes AdS₂ × S² spacetime

$$ds^2 = r_h^2 \delta^2 \frac{dt'^2 + dz'^2}{\sinh^2 \delta z'} + r_h^2 d\Omega_2^2. \quad (9)$$

It is obvious that δ is proportional to the temperature, hence we can define $\delta = 2\pi/\beta$ to introduce the finite-temperature AdS₂, as

$$ds^2 = r_h^2 \frac{4\pi^2}{\beta^2} \frac{dt'^2 + dz'^2}{\sinh^2(2\pi z'/\beta)}. \quad (10)$$

For the Einstein-Maxwell system, it has the action:

$$I = \frac{1}{16\pi G} \int d^4x \sqrt{-g} (R - F_{\mu\nu} F^{\mu\nu}). \quad (11)$$

Doing the dimensional reduction as in [13], and integrating out the Maxwell field, which does not interact with the scalar field considered in this paper, we will get the two-dimensional action:

$$I_{2d} = \frac{\Phi_0}{16\pi G} \left(\int_{M_2} d^2x \sqrt{g^{2d}} R^{2d} - 2 \int_{\partial M_2} dt \sqrt{h} K \right) - \frac{1}{16\pi G} \left(\int_{M_2} d^2x \sqrt{g^{2d}} \Phi (R^{2d} + 2) - 2 \int_{\partial M_2} dt \sqrt{h} \Phi_b K \right), \quad (12)$$

where the $\Phi_0 + \Phi$ is the total dilaton. Φ_0 is a constant and is of leading order, while Φ is of first order, and the Φ_b is the boundary dilaton. The first term is purely topological, according to the Gauss-Bonnet theorem. The second term is the Jackiw-Teitelboim (JT) gravity, where Φ is called the dilaton.

From AdS/CFT correspondence [18, 19], the AdS₂ spacetime has a one-dimensional dual theory. For the AdS₂-JT gravity, the dual theory is the Schwarzian action, as discussed in the next subsection. For the AdS₂-JT gravity, we can first do the path integral of the dilaton field, leading to the fixed AdS radius. For a fixed AdS radius spacetime, the metric can be solved as two functions, and the quantum fluctuation of the metric appears in these functions. However, we can also use another perspective to regard these functions as coordinate transformations. But according to the AdS/CFT correspondence, the quantum gravity of the AdS₂ spacetime at IR should be determined by a cutoff at the boundary. In the passive perspective (the latter one), we can regard the quantum fluctuation of the metric as a reparametrization of the boundary curve.

B. Schwarzian Modes for AdS₂-JT Gravity

Considering the two-dimensional geometry, since the curvature will determine the metric locally, the AdS₂

spacetime is locally the same, and the AdS₂ spacetime has a full reparametrization symmetry. However, if considering the quantum fluctuations, the IR theory of the AdS₂ spacetime is labeled by the boundary curve, which breaks the reparametrization symmetry [7]. Hence, integrating over quantum fluctuations of the metric becomes integrating over the boundary reparametrization modes, which are called the Schwarzian modes. To show how this works, we first consider the AdS₂ spacetime in the Poincaré patch, the metric is given by

$$ds^2 = \frac{dt^2 + dz^2}{z^2}, \quad (13)$$

with the boundary cutoff curve parametrized by $u \in [0, \beta]$, and at the boundary, the induced metric is given by $h_{uu} = \frac{1}{\varepsilon^2} + o(\varepsilon^{-2})$, where $\varepsilon \rightarrow 0$. Consequently, the boundary cutoff curve is given by $z(u) = \varepsilon t'(u)$. Then, the extrinsic curvature is the Schwarzian derivative, i.e.

$$K = 1 + \varepsilon^2 \text{Sch}(t, u) + o(\varepsilon^2), \quad (14)$$

with

$$\text{Sch}(t, u) = -\frac{1}{2} \left(\frac{t''}{t'} \right)^2 + \left(\frac{t'''}{t'} \right)'. \quad (15)$$

The first term of the extrinsic curvature is a constant that can be canceled by a counterterm expressed as the integral of the boundary dilaton along the cutoff curve.

Integrating out the dilaton field Φ , we obtain

$$Z = \int [Dg][D\Phi] e^{-I[g, \Phi]} = \int [Dg] \delta(R + 2) e^{-\frac{1}{8\pi G} \int_{\partial M_2} du \Phi_b \text{Sch}(t, u)}, \quad (16)$$

which fixes the scalar curvature of the quantum fluctuating AdS₂ spacetime, as discussed later.

By the chain rule of the Schwarzian derivative, we can define another reparametrization $du_b = \bar{\Phi}_b du / \Phi_b$ such that Φ_b becomes a constant at the boundary, similar to the discussion in [20]. Redefining $\bar{\Phi}_b = 8\pi G C$, the partition function is totally governed by the Schwarzian derivative:

$$Z = \int [Dg] \delta(R + 2) e^{-C \int_{\partial M_2} du \text{Sch}(t, u)}. \quad (17)$$

Then, we can see that the gravitational effect of the AdS₂ spacetime is governed by the Schwarzian derivative. Hence, considering the conformal gauge, we take the ansatz:

$$ds^2 = -e^{2\omega(x^\pm)} dx^+ dx^-, \quad (18)$$

where the light-cone coordinates are given by $x^\pm = it \pm z$. The scalar curvature is given by

$$R = 8e^{-2\omega} \partial_+ \partial_- \omega. \quad (19)$$

Fixing the scalar curvature to be -2 , we finally obtain the Liouville's equation for ω

$$4\partial_+ \partial_- \omega + e^{2\omega} = 0, \quad (20)$$

whose solution is given by two functions $X^+(x^+)$ and $X^-(x^-)$:

$$e^{2\omega} = \frac{4\partial_+ X^+(x^+) \partial_- X^-(x^-)}{(X^+(x^+) - X^-(x^-))^2}. \quad (21)$$

Thus, different choices of the function X^+ and X^- represent the quantum fluctuations on the AdS₂ spacetime,

reparametrizing the light-cone coordinates x^\pm to X^\pm . For the AdS₂ spacetime from the dimensional reduction of the RN black hole, the two functions should be the same

$$X^+(x) = X^-(x) = F(x) = \frac{\beta}{\pi} \tanh \frac{\pi}{\beta} x, \quad (22)$$

then the AdS₂ spacetime is given by

$$ds^2 = -\frac{4\pi^2}{\beta^2} \frac{dx^+ dx^-}{\sinh^2(\frac{\pi}{\beta}(x^+ - x^-))}. \quad (23)$$

as expected in (10). To compactify the coordinates, we may introduce ‘‘complex light-cone coordinates’’, such that

$$ds^2 = -\frac{4\pi^2}{\beta^2} \frac{dudv}{\sin^2(\frac{\pi}{\beta}(u - v))}. \quad (24)$$

In that case, we can perform a field redefinition, $t = \tan \frac{\pi}{\beta} f(u)$, then the Schwarzian action becomes

$$I = -C \int_0^\beta du \left(\frac{f'''(u)}{f'(u)} - \frac{3}{2} \frac{f''(u)^2}{f'(u)^2} + \frac{2\pi^2}{\beta^2} f'(u)^2 \right). \quad (25)$$

For this action, we can introduce an auxiliary field ψ , and the action then possesses a supersymmetry, allowing it to be one-loop exact, as shown in [8]. After the introducing

the auxiliary ψ , the Schwarzian action becomes

$$I = \frac{C}{2} \int_0^\beta du \left[\left(\frac{f''}{f'} \right)^2 - \frac{4\pi^2}{\beta^2} (f')^2 + \frac{\beta^2}{4\pi^2} \frac{\psi'' \psi'}{f'^2} - \psi' \psi \right]. \quad (26)$$

We can apply the perturbation theory to this model. Since $\tau \sim \tau + \beta$, we can always employ mode expansions on τ and ψ :

$$f = u + g\epsilon(u) = \tau + g \sum_{|n| \geq 2} \frac{\beta}{2\pi} \epsilon_n e^{-i2\pi n u / \beta}, \quad (27)$$

$$\psi = g \sum_{|n| \geq 2} \sqrt{\frac{\beta}{2\pi}} \psi_n e^{-i2\pi n u / \beta}. \quad (28)$$

The terms only containing $\sim \epsilon'(u)$ are total derivative terms; hence, they vanish after integration by parts. Therefore, we can get the following action:

$$I = I^{(0)} + I^{(2)} + gI^{(3)} + g^2 I^{(4)} + O(g^3), \quad (29)$$

where

$$I^{(0)} = -\frac{2\pi^2 C}{\beta}, \quad (30)$$

$$I^{(2)} = \frac{C}{2} \int d\tau \left[(\epsilon'')^2 - \frac{4\pi^2}{\beta^2} (\epsilon')^2 + \frac{\beta^2}{4\pi^2} \psi'' \psi' - \psi' \psi \right], \quad (31)$$

$$I^{(3)} = \frac{C}{2} \int d\tau \left[-2(\epsilon'')^2 \epsilon' - 2\frac{\beta^2}{4\pi^2} \psi'' \psi' \epsilon' \right], \quad (32)$$

$$I^{(4)} = \frac{C}{2} \int d\tau \left[3(\epsilon')^2 (\epsilon'')^2 + 3\frac{\beta^2}{4\pi^2} (\epsilon')^2 \psi'' \psi' \right]. \quad (33)$$

Let us first calculate the action in the momentum space:

$$I^{(2)} = \frac{4\pi^2 C}{\beta} \sum_{|n| \geq 2} n^2 (n^2 - 1) \epsilon_{-n} \epsilon_n - iC \sum_{|n| \geq 2} n(n^2 - 1) \psi_{-n} \psi_n, \quad (34)$$

$$I^{(3)} = i \frac{4\pi^2 C}{3\beta^2} \sum_{|n|, |m|, |n+m| \geq 2} mn(m+n)(m^2 + mn + n^2) \epsilon_{-m-n} \epsilon_m \epsilon_n \\ + \frac{C}{3} \sum_{|n|, |m|, |n+m| \geq 2} nm(m+n)(n+2m) \psi_{-m-n} \psi_m \epsilon_n, \quad (35)$$

$$I^{(4)} = -\frac{\pi^2 C}{\beta^2} \sum_{\text{all modes} \geq 2} mnp(m+n+p)(m^2 + n^2 + p^2 + mn + mp + np) \epsilon_{-m-n-p} \epsilon_m \epsilon_n \epsilon_p \\ + i \frac{3C}{2} \sum_{\text{all modes} \geq 2} mnp(m+n+p)(m+n+2p) \psi_{-m-n-p} \psi_p \epsilon_m \epsilon_n. \quad (36)$$

Here, we have symmetrized bosonic modes and antisymmetrized fermionic modes. Hence, the Feynman rules of the Schwarzian action are given as follows. First, the free propagators are

$$\epsilon_{-n} \text{---} \epsilon_n = \frac{1}{2\pi i} \frac{1}{n^2(n^2 - 1)}, \quad \psi_{-n} \text{---} \psi_n = \frac{1}{2\pi i} \frac{1}{n(n^2 - 1)}. \quad (37)$$

Performing the inverse Fourier transform, we will get the tree-level propagators of ϵ as

$$\begin{aligned} \langle \epsilon(u)\epsilon(0) \rangle &= \left(\frac{\beta^2}{2\pi}\right)^2 \sum_{|n|\geq 2} \langle \epsilon_{-n}\epsilon_n \rangle e^{-2\pi i n u/\beta} = \frac{1}{2\pi C} \left(\frac{\beta}{2\pi}\right)^2 \sum_{|n|\geq 2} e^{-2\pi i n u/\beta} \frac{1}{n^2(n^2-1)} \\ &= \frac{1}{2\pi C} \left(\frac{\beta}{2\pi}\right)^3 \left[1 + \frac{5}{2} \cos \frac{2\pi u}{\beta} - \text{Li}_2(e^{-2\pi i u/\beta}) - \text{Li}_2(e^{2\pi i u/\beta}) \right. \\ &\quad \left. + i(\log(1 - e^{-2\pi i u/\beta}) - \log(1 - e^{2\pi i u/\beta})) \sin \frac{2\pi u}{\beta} \right], \end{aligned} \quad (38)$$

where $\text{Li}_2(x)$ is the polylogarithm function defined as

$$\text{Li}_s(z) = \sum_{n=1}^{\infty} \frac{z^n}{n^s}. \quad (39)$$

From the properties of the polylogarithm function $\text{Li}_2(\frac{1}{y}) + \text{Li}_2(y) = \frac{\pi^2}{3} - \frac{1}{2} \log^2 y - i\pi \log y$, and $\log(1 - e^{-ix}) - \log(1 - e^{ix}) = -ix + \log(e^{ix} - 1) - \log(1 - e^{ix}) = -ix + i\pi$ we obtain:

$$\langle \epsilon(u)\epsilon(v) \rangle \approx \frac{1}{2\pi C} \left(\frac{\beta}{2\pi}\right)^3 \left[1 + \frac{\pi^2}{6} + \frac{5}{2} \cos \frac{2\pi(u-v)}{\beta} + \frac{1}{2} \left(\frac{2\pi(u-v)}{\beta} - \pi \right)^2 + \left(\frac{2\pi(u-v)}{\beta} - \pi \right) \sin \frac{2\pi(u-v)}{\beta} \right]. \quad (40)$$

From the interaction term, we can read off vertices; for instance, the three-point vertices of bosonic and fermionic fields, as well as the four-point vertices of bosonic and fermionic fields, are shown in Fig. 1 and Fig. 2, respectively.

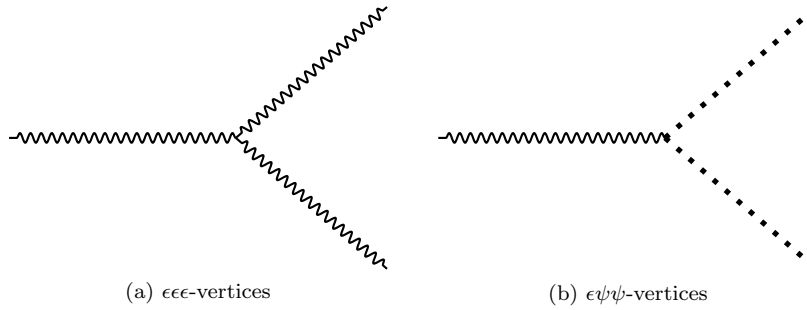


FIG. 1: 3-point vertices of the Schwarzian action

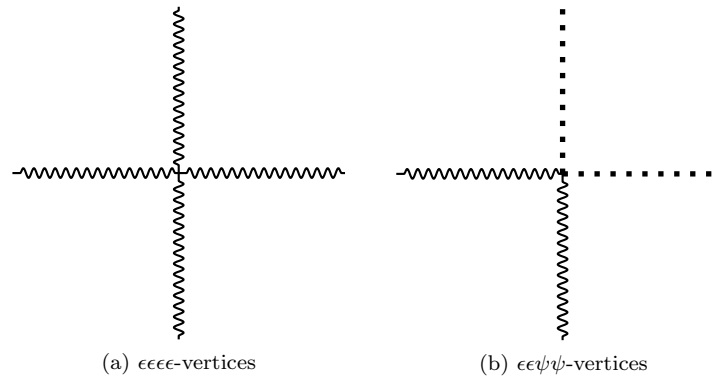


FIG. 2: 4-point vertices of the Schwarzian action

Calculating the one-loop two-point function of the reparametrization, [9] showed that after considering the fermionic loop, the two-point functions may be written in the momentum space as

$$\langle \epsilon_{-n}\epsilon_n \rangle_{\text{cubic}} = \begin{cases} \frac{g^2}{8\pi^2} \frac{-112+104n^2+179n^4-111n^6+12n^8}{n^2(n^2-4)^2(n^2-1)^2}, & n \neq 2, \\ -\frac{g^2}{96} + \frac{1465g^2}{6912\pi^2}, & n = 2, \end{cases} \quad (41)$$

$$\langle \epsilon_{-n} \epsilon_n \rangle_{\text{quartic}} = -\frac{9g^2}{8\pi^2} \frac{1}{(n^2 - 1)^2}, \quad (42)$$

which remain finite after the inverse Fourier transform.

In this case, we can calculate the quantum corrections to the quantities in the AdS₂ spacetime. For the

AdS₂ metric, we can expand the metric in terms of the Schwarzian modes ϵ 's. Up to the quadratic order in ϵ , the metric is

$$\begin{aligned} ds^2 &= -\frac{4\pi^2}{\beta^2} \frac{f'(x^+)f'(x^-)}{\sin^2\left(\frac{\pi}{\beta}(f(x^+) - f(x^-))\right)} dx^+ dx^- \\ &= -\frac{4\pi^2}{\beta^2} \frac{(1 + \epsilon'(x^+))(1 + \epsilon'(x^-))}{\sin^2\left(\frac{\pi}{\beta}((x^+ - x^-) + (\epsilon(x^+) - \epsilon(x^-)))\right)} dx^+ dx^- \\ &= -\frac{4\pi^2}{\beta^2} \frac{dx^+ dx^-}{\sin^2\left(\frac{\pi}{\beta}(u - v)\right)} (1 + \epsilon'(x^+) + \epsilon'(x^-) + \frac{2\pi}{\beta} \cot\left(\frac{\pi(x^+ - x^-)}{\beta}\right) (\epsilon(x^+) - \epsilon(x^-))) \\ &\quad + \frac{1}{2\beta^2} \frac{1}{2\sin^2\frac{\pi}{\beta}(u - v)} \left[4\pi^2 (\epsilon(u) - \epsilon(v))^2 + \beta^2 \epsilon'(u)\epsilon'(v) - 2\pi\beta \sin\left(\frac{2\pi(x^+ - x^-)}{\beta}\right) (\epsilon'(x^+) + \epsilon'(x^-)) (\epsilon(x^+) - \epsilon(x^-)) \right. \\ &\quad \left. + \cos\left(\frac{2\pi(x^+ - x^-)}{\beta}\right) (2\pi(\epsilon(x^+) - \epsilon(x^-))^2 - \beta^2 \epsilon'(x^+)\epsilon'(x^-)) \right]. \end{aligned} \quad (43)$$

Similar to the quantization law in quantum mechanics, we need to represent a classical operator AB as $\frac{1}{2}(AB + BA)$, which makes the quantum metric operator symmetric in x^+ and x^- .

C. Quantum-Corrected Scalar Equation of Motion

In this section, we will derive the quantum correction to the scalar field equation in the RN black hole.

As derived in Sec. II A, the near-horizon region of the near-extremal RN black hole is AdS₂ × S². From the dimensional reduction, we will get the JT gravity, which plays the role of the effective action for gravity. Even though the AdS₂ region is located in the near-horizon region, we can still receive the correction for the far-away region. First, the near-horizon region and the far-away region share the same boundary, i.e., the overlapping region. Hence, the equation of motion could be matched in the overlapping region, resulting in the far-away region having the same form of fluctuations as the Schwarzian modes. In that case, the expression of the quantum correction could be carried to the far-away region. Secondly, since the boundary conditions can be matched if they apply to the same equation, if the fields in the RN black hole background are affected by the quantum fluctuations in the near-horizon region, it should also carry information to the far-away region. In addition, it is not hard to find that the correction to the metric vanishes if we take

the near-boundary limit $2z = x^+ - x^- \rightarrow 0$. Hence, we can calculate the quantum correction in the near-horizon AdS₂ region, and then extend it to the far-away region, which gives us the quantum fluctuations in the whole RN black hole. In the discussion of Sec. III A, we will show that for the scalar quasi-normal modes, the only difference between the classical and the quantum-corrected RN black holes is the effective potential, while the boundary conditions on both sides will not be changed, neither does the light ring, the maximum point of the effective potential. Therefore, the global property of the scalar quasi-normal mode equation remains unchanged.

In that case, the Schwinger-Dyson equation [21, 22] for the matter field Ψ in the RN black hole should be calculated in the following steps,

$$\begin{aligned} \frac{1}{Z} \frac{\delta Z}{\delta \Psi} &= \frac{1}{Z} \int [d\Psi] [dg_{4d}] \frac{\delta I_{\text{mat}}}{\delta \Psi} e^{-I_{\text{gra}}[g] - I_{\text{mat}}[g, \Psi]} \\ &= \frac{1}{Z} \int [d\Psi] [d\Phi] [dg_{2d}] \frac{\delta I_{\text{mat}}}{\delta \Psi} e^{-I_{\text{gra}}[g, \Phi] - I_{\text{mat}}[g, \Psi]} \\ &= \frac{1}{Z} \int [d\Psi] [dg_{2d}] \delta(R + 2) \frac{\delta I_{\text{mat}}}{\delta \Psi} e^{-I_{\text{gra}}[g_{2d}, \Phi] - I_{\text{mat}}[g_{2d}, \Psi]} \\ &= \frac{1}{Z} \int [d\Psi] [d\epsilon] \frac{\delta I_{\text{mat}}}{\delta \Psi} e^{-I_{\text{Schwarzian}}[\epsilon] - I_{\text{mat}}[g_{2d}(\epsilon), \Psi]} \\ &= \left\langle \frac{\delta I_{\text{matter}}}{\delta \Psi} \right\rangle, \end{aligned} \quad (44)$$

which means that we should first write the metric as a

function of the Schwarzian modes, like in Eq. (43). Then, we can regard it as a given metric and derive the equation of motion for the matter fields. Finally, we should average the matter equation of motion within the path integral over the Schwarzian modes, which will eventually provide us with the quantum-corrected equation of motion. In principle, this equation is not equivalent to the classical equation of motion for a matter field in the quantum-corrected metric. However, these two treatments coincide at the leading order in quantum correction for a neural scalar field, in the same spirit as the Ehrenfest theorem in quantum mechanics [23].

For the free massless real scalar field, we can take the ansatz as:

$$\Psi(r) = \sum_{l,m,\omega} \frac{R(r)}{r} e^{-i\omega t} Y_{lm}(\theta, \varphi). \quad (45)$$

Then, for any spherically-symmetric metric, we can write it as $ds^2 = -F(r)dt^2 + G(r)dr^2 + r^2d\theta^2 + r^2\sin^2\theta d\varphi^2$.

Hence, the equation of motion of the scalar field becomes:

$$\frac{1}{\sqrt{F(r)G(r)r^2}} \left(-\partial_t r^2 \sqrt{\frac{G(r)}{F(r)}} \partial_t + \partial_r r^2 \sqrt{\frac{F(r)}{G(r)}} \partial_r \right) \Psi - \frac{l(l+1)}{r^2} \Psi = 0. \quad (46)$$

For the metric of the form (43), we see that the metric components have the form:

$$F(r) = \left(1 - \frac{2M}{r} + \frac{Q^2}{r^2} \right) A_{\text{cor}} = f(r) A_{\text{cor}}, \quad (47)$$

$$G(r) = \frac{A_{\text{cor}}}{1 - \frac{2M}{r} + \frac{Q^2}{r^2}} = \frac{A_{\text{cor}}}{f(r)}.$$

Hence, the scalar field equation in the radial direction becomes:

$$0 = \frac{1}{r} \frac{d}{dr} \left(f(r) \frac{d}{dr} R_{lm}(r) \right) + \left(\frac{1}{r f(r)} \omega^2 - A_{\text{cor}} \frac{l(l+1)}{r^3} - \frac{f'(r)}{r^2} \right) R_{lm}(r), \quad (48)$$

where the correction factor is given as

$$A_{\text{cor}} = \sin^2 \left(\frac{\pi}{\beta} ((x^+ - x^-)) \right) \times \left[\frac{(1 + \epsilon'(x^+))(1 + \epsilon'(x^-))}{\sin^2 \left(\frac{\pi}{\beta} ((x^+ - x^-) + (\epsilon(x^+) - \epsilon(x^-))) \right)} \right]$$

$$= 1 + \epsilon'(x^+) + \epsilon'(x^-) + \frac{2\pi}{\beta} \cot \left(\frac{\pi(x^+ - x^-)}{\beta} \right) (\epsilon(x^+) - \epsilon(x^-))$$

$$+ \frac{1}{2\beta^2} \frac{1}{2 \sin^2 \frac{\pi}{\beta} (x^+ - x^-)} \left[4\pi^2 (\epsilon(x^+) - \epsilon(x^-))^2 + \beta^2 \epsilon'(x^+) \epsilon'(x^-) \right] \quad (49)$$

$$- 2\pi\beta \sin \left(\frac{2\pi(x^+ - x^-)}{\beta} \right) (\epsilon'(x^+) + \epsilon'(x^-)) (\epsilon(x^+) - \epsilon(x^-))$$

$$+ \cos \left(\frac{2\pi(x^+ - x^-)}{\beta} \right) (2\pi(\epsilon(x^+) - \epsilon(x^-))^2 - \beta^2 \epsilon'(x^+) \epsilon'(x^-)) \left. \right].$$

Here, x^+ and x^- are the light-cone coordinates for the reduced AdS₂ spacetime. Putting this equation into the

path integral, we obtain the quantum-averaged correction factor $\langle A_{\text{cor}} \rangle$ as:

$$\langle A_{\text{cor}} \rangle = 1 + \frac{\beta}{32\pi^4 C} (r - r_+) (r - r_-) \left[6\pi^2 \ln^2 \frac{r - r_-}{r - r_+} + (6\pi^2 + 4\pi^2 \ln^2 \frac{r - r_-}{r - r_+}) \frac{(2\pi/\beta)^2}{(r - r_+) (r - r_-)} \right]$$

$$- 6\beta\pi \ln \frac{r - r_-}{r - r_+} \frac{(2\pi/\beta)(r - r_h)}{(r - r_+) (r - r_-)}. \quad (50)$$

Finally, we obtain the radical equation of motion for

the scalar field after quantum correction

$$0 = \frac{1}{r} \frac{d}{dr} \left(f(r) \frac{d}{dr} R_{lm}(r) \right) + \left(\frac{1}{r f(r)} \omega^2 - \langle A_{\text{cor}} \rangle \frac{l(l+1)}{r^3} - \frac{f'(r)}{r^2} \right) R_{lm}(r). \quad (51)$$

D. Evaluation of the Boundary Dilaton

For the AdS₂ JT gravity, assuming the boundary dilaton field is a constant, it can be viewed as a free parameter. However, this is not right for the AdS₂ near-horizon region of the RN black hole. In [13], considering the Schwarzsian action correction, the entropy of the RN black hole is given by

$$S = S_0 + 4\pi^2 \bar{\Phi}_b T + \frac{3}{2} \log(\bar{\Phi}_b T) + O(T^2), \quad (52)$$

while from the classical black hole thermodynamics, we obtain the semiclassical entropy as

$$S = \frac{A_H}{4} = \pi r_+^2 = \pi M^2 + 8\pi^2 M^3 T + O(T^2). \quad (53)$$

In the high-temperature limit, the logarithmic term is subleading, and hence, comparing the terms linear in temperature, which is the capacity of the black hole, it can be deduced that the boundary dilaton field is given by

$$\bar{\Phi}_b = 2M^3. \quad (54)$$

Since the boundary dilaton $\bar{\Phi}_b$ is proportional to the coupling C , the strength of the quantum correction is determined by the mass of the black hole:

$$C \sim M^3. \quad (55)$$

Meanwhile, the expression of the quantum-corrected entropy gives us the effective range for our discussion. The lower bound of the entropy is $-\infty$, and in our discussion, the temperature of the RN black hole could not be so low that the entropy is negative. Therefore, our discussion has three requirements: (1) It is a near-extremal RN black hole, i.e., the temperature T should be smaller than that of a Schwarzschild black hole with the same mass, i.e., $T \ll 8\pi M$; (2) The perturbative expansion is suitable, i.e., $\beta/C \ll 1$; (3) The quantum-corrected entropy should be positive, i.e., the entropy given in (52) is positive.

III. CALCULATION OF SCALAR QNMS

A. Basic Discussion on Scalar Quasi-Normal Modes

For the scalar field equation, using the tortoise coordinates $x = \int dr/f(r)$. Then, the equation of motion for the scalar field becomes:

$$-\frac{d^2}{dx^2} R_{lm} + (V(r_*) - \omega^2) R_{lm} = 0, \quad (56)$$

where the effective potential is given by

$$V(r) = f(r) \left(\frac{l(l+1)}{r^2} \langle A_{\text{cor}} \rangle + \frac{f'(r)}{r} \right). \quad (57)$$

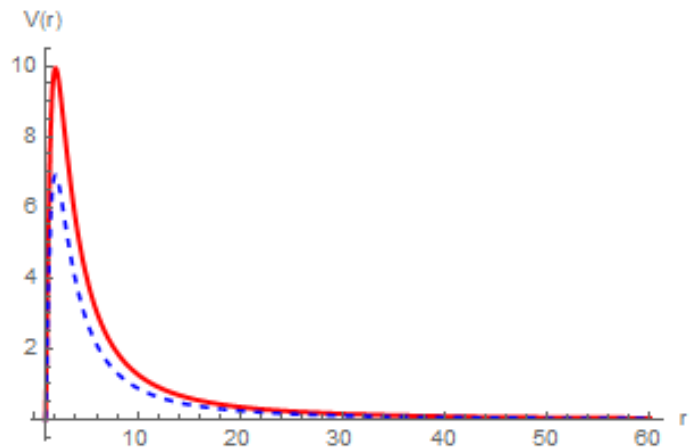


FIG. 3: The effective potential. The blue line and the red line represent the classical and the quantum-corrected effective potentials for the scalar field, respectively, in the RN black hole background.

The corrected potential and the original RN case are shown in Fig. 3.

The effective potential after correction has a similar property to the classical case. First, the effective potential vanishes at the horizon $r = r_+$ and at infinity $r = \infty$. Additionally, the effective potential has only one peak, and numerical calculations reveal that the maximum position is nearly identical to the original RN case. Hence, this equation is an eigenvalue problem, determining the discrete spectrum of ω . We have the boundary conditions at the horizon and infinity as

$$\begin{aligned} R &\rightarrow e^{-i\omega x}, & x &\rightarrow -\infty, \\ R &\rightarrow e^{i\omega x}, & x &\rightarrow \infty, \end{aligned} \quad (58)$$

which impose the ingoing boundary condition at the horizon and the outgoing boundary condition at the future infinity.

Several methods have been developed for determining QNMs, including the Wentzel-Kramers-Brillouin (WKB) method [24], continuous fraction method [25], Prony method [26], spectral method [27], and so forth. Among these methods, the WKB method has been developed in numerous papers, ranging from the 1st order to the 13th order. However, it is important to note that the higher-order WKB method does not necessarily imply higher accuracy. In later calculations, we find that the 3rd- and 4th-order WKB results are the most stable ones, having very small errors compared to the results given by the Prony method (see App. A 1). Therefore, we will use the 3rd-order WKB method and the Prony method to obtain the QNMs in our work. In the following two subsections, we will introduce these two methods.

B. WKB Method

For the Schrödinger-like equation in tortoise coordinate x ,

$$\frac{d^2 R}{dx^2} + [\omega^2 - V(x)] R = 0, \quad (59)$$

there is a maximum point at $x = x_0$

$$\left. \frac{dV}{dx} \right|_{x=x_0} = 0, \quad V_0 = V(x_0). \quad (60)$$

Hence, the effective potential can be approximated by the power series

$$V(x) = V_0 + \frac{1}{2} V''(x_0)(x - x_0)^2 + \dots \quad (61)$$

There will be two transition points,

$$V(x_1) = V(x_2) = \text{Re}(\omega^2), \quad (62)$$

where the wave function undergoes transitions in its exponential decay and trigonometric oscillation behaviors. To simplify the equation, we introduce a new variable $z = \sqrt{V''(x_0)/2}(x - x_0)$ and $z_0^2 = V_0 - \omega^2$. To the first order, the wave equation becomes the standard Airy equation, whose solution is given by a superposition of the Airy functions:

$$R = C_1 \text{Ai}(z) + C_2 \text{Bi}(z). \quad (63)$$

However, to match the boundary condition at the far-away region requires $C_2 = 0$. In addition, matching the solutions will lead to the Bohr-Sommerfeld condition:

$$\int_{x_1}^{x_2} \sqrt{\omega^2 - V(x)} dx = \left(n + \frac{1}{2} \right) \pi, \quad (64)$$

which gives us the first-order WKB approximation as:

$$i \frac{\omega^2 - V_0}{\sqrt{-2V''(x_0)}} = n + \frac{1}{2}, \quad (65)$$

where n is an integer named the overtone number of the quasi-normal modes.

Using perturbation theory in quantum mechanics, we can obtain higher-order results, as in [24, 28, 29].

C. Prony Method

Besides the WKB approximation method, we can also obtain the quasi-normal modes from the time evolution of the fields, which was first developed in [30]. For the time-dependent Schrödinger-like equation, we can write it as

$$-\frac{\partial^2 \Psi(t, x)}{\partial t^2} + \frac{\partial^2 \Psi(t, x)}{\partial x^2} = V(x) \Psi(t, x). \quad (66)$$

Introducing the light-cone coordinates $u = t + x$ and $v = t - x$, we obtain

$$\partial_u \partial_v \Psi(u, v) = -V \Psi(u, v). \quad (67)$$

Suppose there is a lattice such that $\Psi_{ij} = \Psi(u_0 + ih, v_0 + jh)$. Rewriting the derivative as a finite difference

$$\begin{aligned} \frac{d\Psi_{i,j}}{du} &= \frac{\Psi_{i+1,j} - \Psi_{i-1,j}}{2h}, \\ \frac{d\Psi_{i,j}}{dv} &= \frac{\Psi_{i,j+1} - \Psi_{i,j-1}}{2h}, \end{aligned} \quad (68)$$

redefining $\Psi_{i+1,j+1} \rightarrow \Psi_N, \Psi_{i-1,j-1} \rightarrow \Psi_S, \Psi_{i+1,j-1} \rightarrow \Psi_E, \Psi_{i-1,j+1} \rightarrow \Psi_W$, and using the central rule as

$$\Psi_{i,j} = \frac{\Psi_W + \Psi_E}{2} = \frac{\Psi_{i+1,j-1} + \Psi_{i-1,j+1}}{2}, \quad (69)$$

we obtain a finite difference equation

$$\Psi_N = \Psi_W + \Psi_E - \Psi_S - 4h^2 V_{ij} \frac{\Psi_W + \Psi_E}{2}. \quad (70)$$

Given any initial data on an equal- u surface, for instance, the Gaussian wave packet $\Psi(0, v) = \exp(-(v - v_0)^2/\sigma^2)$, we can get Ψ for any u and v . For example, the following two figures show the time evolution of the scalar with or without quantum corrections.

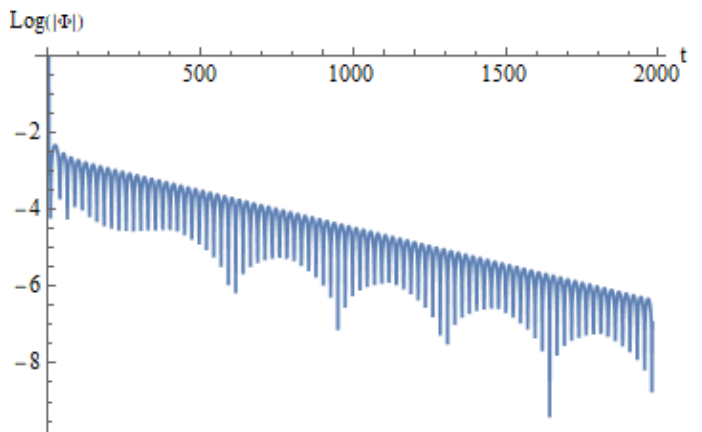


FIG. 4: The time evolution of the scalar field in the RN black hole background without quantum correction

We can transform the light-cone coordinates back to the spacetime coordinates. In that case, the time evolution can be written as:

$$x_j = \Psi(t_0 + jh) = \sum_{n=1}^p A_n z_n^j, \quad (71)$$

where $A_n = C_n e^{-i\omega_n t_0}$ is the initial data of the time evolution. Hence, we can obtain the quasi-normal modes through $z_n = \exp(-i\omega_n h)$. Consider a polynomial

$$P(z) = \prod_{n=1}^p (z - z_n), \quad (72)$$

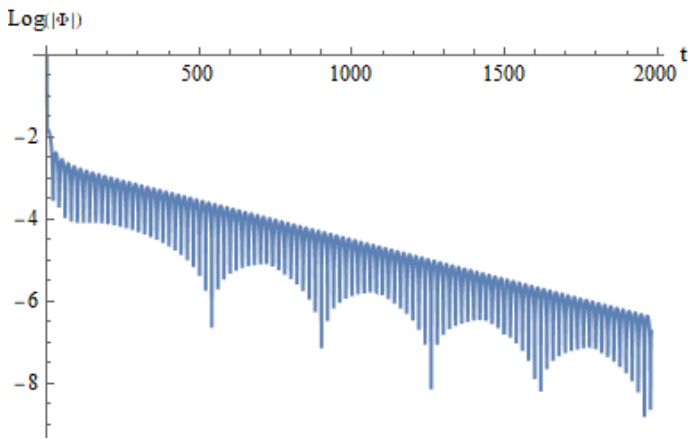


FIG. 5: The time evolution of the scalar field in the RN black hole ground with quantum correction

which can be expanded to a degree p polynomial

$$P(z) = \sum_{n=0}^p \alpha_n z^{p-n}, \quad (73)$$

where the zeros of this polynomial are given by the z_n 's. It is not hard to show that:

$$\begin{aligned} \sum_{n=0}^p \alpha_n x_{m-n} &= \sum_{n=0}^p \alpha_n \sum_{k=1}^p A_k z_k^{m-n} \\ &= \sum_{k=1}^p A_k z_k^{m-p} \sum_{n=0}^p \alpha_n z_k^{m-n} \\ &= \sum_{k=1}^p A_k z_k^{m-n} P(z = z_k) = 0, \end{aligned} \quad (74)$$

where we have used Eq. (73). Hence, there is a linear equation about $x_m (m \geq p)$

$$x_m = - \sum_{n=1}^p \alpha_n x_{m-n}. \quad (75)$$

Solving this equation, we finally arrive at the quasi-normal modes in which the fundamental mode has the largest amplitudes.

IV. RESULTS OF QUANTUM-CORRECTED SCALAR QUASI-NORMAL MODES

To see the effects of the mass and the charge-mass ratio more clearly, we fix one parameter and change the other parameter, and then we obtain the results shown in Fig. 6, 7, 8 and for detailed data, see App. A 2.

First, the quasi-normal modes are modified by the quantum correction to the equation of motion. In particular, the real parts of the quasi-normal modes have much larger quantum corrections than the imaginary parts.

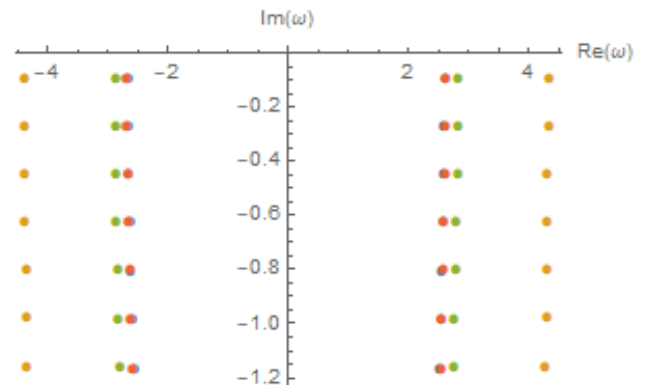


FIG. 6: Quasi-normal modes of the scalar field with fixed charge-mass ratio $q = 0.9999$, quantum number $l = 10$, and different values of CT . The values of $CT = 10^4, 10^5, 10^6$ are denoted by the yellow, green, and red dots. The red dots almost coincide with the classical results given by the blue dots.

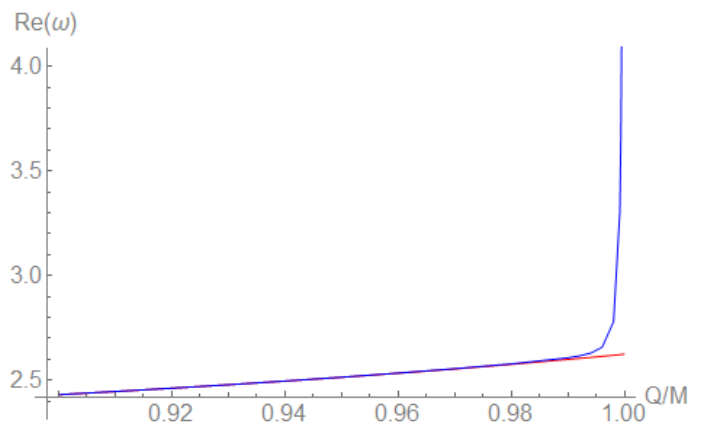


FIG. 7: The real part of quasi-normal modes as a function of Q/M with a given mass $M = 1$ kg. The red and the blue curves denote the classical and the quantum-corrected results, respectively.

When the black hole becomes more extremal, in other words, the temperature is lower, the quantum correction becomes stronger. From dimensional analysis, CT is proportional to the $\frac{\delta}{M} \times M^2 \times 10^5$ with the mass unit kg. In that case, when the mass is about 10^{-3} kg, the quantum correction is so strong that the perturbation theory breaks down. In that case, quantum gravity is needed when analyzing this phenomenon.

V. DISCUSSION AND OUTLOOK

In this paper, we introduce the quantum gravity correction to the scalar field in the RN black hole background and discuss its quasi-normal modes. With the 2d JT gravity/1d Schwarzian theory correspondence, the effective equation of motion for the scalar field can be

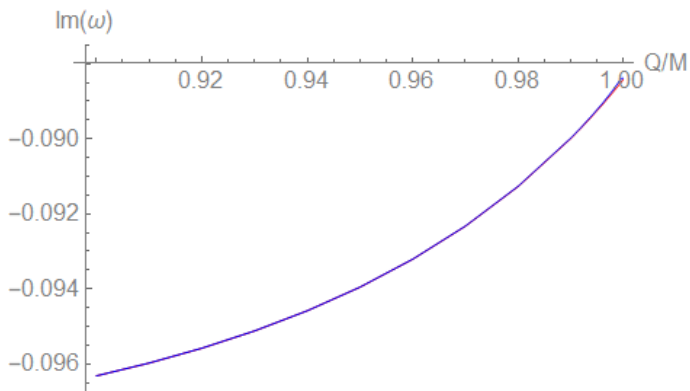


FIG. 8: The imaginary part of quasi-normal modes as a function of Q/M with the given mass $M = 1$ kg. The red and blue curves denote the classical and the quantum-corrected results, respectively.

calculated by the path integral over all reparametrization modes.

In comparison to the original scalar quasi-normal modes in the RN black hole background, the only difference is the effective potential in the quantum correction equation. It can be seen that the quasi-normal modes differ from the uncorrected case. Compared with the classical modes, the quantum correction should be large if the temperature is low or the mass is small. For the quasi-normal modes, the real part is very sensitive to the quantum correction, while the imaginary part is not. In our discussion, if $CT < 1$, the quantum correction becomes very large, but it should be noted that here we use the perturbative expansion of the Schwarzschild modes, and hence, the $CT < 1$ results are not valid in this limit. The exact quantum correction of the RN black hole should be carried out in non-perturbative methods later, which can be one of the further directions to investigate.

From numerical analysis, for the small mass near-extremal RN black hole, the quasi-normal modes may be completely different from the classical solutions. In that case, our calculation may provide a new perspective on primordial black holes, as their masses could be very small.

In addition, other perturbation fields may also be defined on the RN black hole background, and further calculations can be achieved using our methods, such as spinor fields, vector fields, and tensor fields. The quantum corrections of the RN black hole may cause many other observable effects of physical interest.

ACKNOWLEDGMENTS

We would like to thank Xiao-Long Liu, René Meyer, Run-Qiu Yang, Zhenbin Yang, Amos Yarom, and Cong-Yuan Yue for many helpful discussions. J.N. was par-

tially supported by the NSFC under grants No. 12375067, No. 12147103, and No. 12247103. This work is partially supported by the National Natural Science Foundation of China under grants No. 12375058, No. 12361141825, and No. 12035016, as well as the National Key Research and Development Program of China with Grant No. 2021YFC2203001.

Appendix A: More Details of the Results

1. Different Orders of WKB

As stated in Sec. III B, the higher-order WKB method does not necessarily mean more accuracy. In this appendix, we use the 1-13 order WKB method to evaluate the scalar quasi-normal modes with $M = 10$ kg, $q = 0.9999$, and $l = 10$. It can be seen that for the high-order WKB method, the quasi-normal modes become very unstable; hence, we should not trust these results.

| Order | Corrected | Uncorrected |
|-------|---|--------------------|
| 1 | 3.15307-0.0884334i | 2.62920-0.0884558i |
| 2 | 3.14966-0.0885292i | 2.62511-0.0885936i |
| 3 | 3.14966-0.0884130i | 2.62510-0.0884262i |
| 4 | 3.14987-0.0884071i | 2.62511-0.0884260i |
| 5 | 3.98150-2.43690i | 2.62511-0.0884263i |
| 6 | 0.0404317-239.973i | 2.62511-0.0884262i |
| 7 | 9931.86+9934.76i | 2.62511-0.0884288i |
| 8 | 184.073+536040.2i | 2.62533-0.0884215i |
| 9 | $1.05809 \times 10^7 + 1.05945 \times 10^7 i$ | 2.62546-0.0921458i |
| 10 | $35666.7 + 3.14296 \times 10^9 i$ | 2.74253-0.0882124i |
| 11 | $1.79356 \times 10^{11} + 1.79383 \times 10^{11} i$ | 21.7580-21.5846i |
| 12 | $4.47426 \times 10^{13} + 7.19078 \times 10^8 i$ | 136.716-3.43513i |
| 13 | $1.90853 \times 10^{15} + 1.90800 \times 10^{15} i$ | 1780.12-1774.87i |

TABLE I: Different-order results

From this table, for the classical RN black hole, if we use the WKB method with orders higher than 10, the results also become very large, which implies the failure of the high-order WKB method. For the quantum-corrected case, the failure order becomes lower, even the five-order WKB method causes errors. In that case, to ensure the reliability of the results, we always employ the three-order WKB method.

2. The Comparison of the WKB and the Prony Methods

To show quantum correction on the quasi-normal modes, we take the quantum numbers $l = 1$ and 10 , $n = 0$, and use both methods in the previous section to calculate the quasi-normal modes with different masses and charge-mass ratios.

| Quantum number l | Methods | Corrected or not | quasi-normal modes ω/M | corrections |
|--------------------|---------|------------------|-------------------------------|---|
| $l_1 = 1$ | WKB | NO | 0.350922-0.0971917i | Almost 0 |
| | WKB | YES | 0.350922-0.0971919i | |
| | Prony | NO | 0.352210-0.0967679i | $1.4 \times 10^{-5} + 1.96 \times 10^{-5}i$ |
| | Prony | YES | 0.352224-0.0967875i | |
| $l_2 = 10$ | WKB | NO | 2.43173-0.0963221i | Almost 0 |
| | WKB | YES | 2.43173-0.0963221i | |
| | Prony | NO | 2.43211-0.0962772i | Almost 0 |
| | Prony | YES | 2.43211-0.0962772i | |

TABLE II: Result 1: $M = 1000$ kg, $q = 0.9$

| Quantum number l | Methods | Corrected or not | quasi-normal modes ω/M | corrections |
|--------------------|---------|------------------|-------------------------------|---|
| $l_1 = 1$ | WKB | NO | 0.375416-0.0895061i | $5 \times 10^{-6} - 1.91 \times 10^{-5}i$ |
| | | YES | 0.375421-0.0895252i | |
| | Prony | NO | 0.377334-0.0894164i | $1.6 \times 10^{-5} - 7 \times 10^{-7}i$ |
| | | YES | 0.377350-0.0894171i | |
| $l_2 = 10$ | WKB | NO | 2.62276-0.0885827i | Almost 0 |
| | | YES | 2.62276-0.0885826i | |
| | Prony | NO | 2.62559-0.0883785i | Almost 0 |
| | | YES | 2.62564-0.0883784i | |

TABLE III: Result 2: $M = 1000$ kg, $q = 0.9999$

| Quantum number l | Methods | Corrected or not | quasi-normal modes ω/M | corrections |
|--------------------|---------|------------------|-------------------------------|-------------|
| $l_1 = 1$ | WKB | NO | 0.350922-0.0971917i | Almost 0 |
| | WKB | YES | 0.350922-0.0971915i | |
| | Prony | NO | 0.352224-0.0967875i | Almost 0 |
| | Prony | YES | 0.352220-0.0967915i | |
| $l_2 = 10$ | WKB | NO | 2.43173-0.0963221i | Almost 0 |
| | WKB | YES | 2.43173-0.0963221i | |
| | Prony | NO | 2.43211-0.0962772i | Almost 0 |
| | Prony | YES | 2.43211-0.0962772i | |

TABLE IV: Result 3: $M = 100$ kg, $q = 0.9$

| Quantum number l | Methods | Corrected or not | quasi-normal modes ω/M | corrections |
|--------------------|---------|------------------|-------------------------------|--|
| $l_1 = 1$ | WKB | NO | 0.375675-0.0893758i | $7.36 \times 10^{-4} + 1.07 \times 10^{-5}i$ |
| | WKB | YES | 0.376411-0.0893651i | |
| | Prony | NO | 0.377334-0.0894164i | $7.43 \times 10^{-4} - 7.3 \times 10^{-6}i$ |
| | Prony | YES | 0.378077-0.0894237i | |
| $l_2 = 10$ | WKB | NO | 2.62510-0.0884262i | $5.77 \times 10^{-3} + 1.5 \times 10^{-6}i$ |
| | WKB | YES | 2.63087-0.0884257i | |
| | Prony | NO | 2.62558-0.0883785i | $5.77 \times 10^{-3} + 5 \times 10^{-7}i$ |
| | Prony | YES | 2.63135-0.0883780i | |

TABLE V: Results 4: $M = 100$ kg, $q = 0.9999$

From our results, the WKB and Prony methods yield very close results, indicating that the quantum-gravity-corrected quasi-normal modes differ from the classical ones.

| Quantum number l | Methods | Corrected or not | quasi-normal modes ω/M | corrections |
|--------------------|---------|------------------|-------------------------------|-------------|
| $l_1 = 1$ | WKB | NO | 0.350922-0.0971917i | Almost 0 |
| | WKB | YES | 0.350922-0.0971915i | |
| | Prony | NO | 0.352224-0.0967875i | Almost 0 |
| | Prony | YES | 0.352218-0.0967840i | |
| $l_2 = 10$ | WKB | NO | 2.43173-0.0963221i | Almost 0 |
| | WKB | YES | 2.43173-0.0963221i | |
| | Prony | NO | 2.43211-0.0962772i | Almost 0 |
| | Prony | YES | 2.43211-0.0962772i | |

TABLE VI: Result 5: $M = 10$ kg, $q = 0.9$

| Quantum number l | Methods | Corrected or not | quasi-normal modes ω/M | corrections |
|--------------------|---------|------------------|-------------------------------|----------------------------------|
| $l_1 = 1$ | WKB | NO | 0.375675-0.0893758i | $0.067656+2.904 \times 10^{-4}i$ |
| | WKB | YES | 0.443331-0.0890854i | |
| | Prony | NO | 0.377334-0.0894164i | $0.067288-1.560 \times 10^{-4}i$ |
| | Prony | YES | 0.444622-0.0892604i | |
| $l_2 = 10$ | WKB | NO | 2.62510-0.0884262i | $0.52456+1.32 \times 10^{-5}i$ |
| | WKB | YES | 3.14966-0.0884130i | |
| | Prony | NO | 2.62558-0.0883785i | $0.52490+3.45 \times 10^{-5}i$ |
| | Prony | YES | 3.15048-0.0883440i | |

TABLE VII: Result 6: $M = 10$ kg, $q = 0.9999$

| Quantum number l | Methods | Corrected or not | quasi-normal modes ω/M | corrections |
|--------------------|---------|------------------|-------------------------------|---|
| $l_1 = 1$ | WKB | NO | 0.350922-0.0971917i | $1.6 \times 10^{-5}+3 \times 10^{-7}i$ |
| | WKB | YES | 0.350938-0.0971914i | |
| | Prony | NO | 0.352224-0.0967875i | $1.7 \times 10^{-5}-2.86 \times 10^{-5}i$ |
| | Prony | YES | 0.352241-0.0968161i | |
| $l_2 = 10$ | WKB | NO | 2.43173-0.0963221i | $1.3 \times 10^{-4}+7 \times 10^{-7}i$ |
| | WKB | YES | 2.43186-0.0963214i | |
| | Prony | NO | 2.43211-0.0962772i | $1.3 \times 10^{-4}+7 \times 10^{-7}i$ |
| | Prony | YES | 2.43224-0.0962765i | |

TABLE VIII: Result 7: $M = 1$ kg, $q = 0.9$

| Quantum number l | Methods | Corrected or not | quasi-normal modes ω/M | corrections |
|--------------------|---------|------------------|-------------------------------|-----------------------------------|
| $l_1 = 1$ | WKB | NO | 0.375675-0.0893758i | $2.001312+9.681 \times 10^{-4}i$ |
| | WKB | YES | 2.376987-0.0884077i | |
| | Prony | NO | 0.377334-0.0894164i | $2.000015+1.0478 \times 10^{-3}i$ |
| | Prony | YES | 2.377349-0.0883687i | |
| $l_2 = 10$ | WKB | NO | 2.62510-0.0884262i | $14.97624+4.32 \times 10^{-5}i$ |
| | WKB | YES | 17.60134-0.0883834i | |
| | Prony | NO | 2.62558-0.0883784i | $15.12097+2.2727 \times 10^{-3}i$ |
| | Prony | YES | 17.74655-0.0861057i | |

TABLE IX: Result 8: $M = 1$ kg, $q = 0.9999$

-
- [1] R. A. Konoplya and A. Zhidenko, Quasinormal modes of black holes: From astrophysics to string theory, *Reviews of Modern Physics* **83**, 793–836 (2011).
- [2] M. Maggiore, *Gravitational Waves: Volume 2: Astrophysics and Cosmology* (Oxford University Press, 2018).
- [3] S. Chandrasekhar, *The Mathematical Theory of Black Holes* (Oxford University Press, 1998).
- [4] C. Teitelboim, Gravitation and Hamiltonian Structure in Two Space-Time Dimensions, *Phys. Lett. B* **126**, 41 (1983).
- [5] R. Jackiw, Lower Dimensional Gravity, *Nucl. Phys. B* **252**, 343 (1985).
- [6] A. Almheiri and J. Polchinski, *Models of AdS₂ backreaction and holography* (2015), [arXiv:1402.6334](https://arxiv.org/abs/1402.6334) [hep-th].
- [7] J. Maldacena, D. Stanford, and Z. Yang, *Conformal symmetry and its breaking in two dimensional nearly anti-de-sitter space* (2016), [arXiv:1606.01857](https://arxiv.org/abs/1606.01857) [hep-th].
- [8] D. Stanford and E. Witten, Fermionic localization of the schwarzian theory, *Journal of High Energy Physics* **2017**, [10.1007/jhep10\(2017\)008](https://arxiv.org/abs/10.1007/jhep10(2017)008) (2017).
- [9] Y.-H. Qi, S.-J. Sin, and J. Yoon, Quantum correction to chaos in schwarzian theory, *Journal of High Energy Physics* **2019**, [10.1007/jhep11\(2019\)035](https://arxiv.org/abs/10.1007/jhep11(2019)035) (2019).
- [10] A. Blommaert, T. G. Mertens, and H. Verschelde, Clocks and Rods in Jackiw-Teitelboim Quantum Gravity, *JHEP* **09**, 060, [arXiv:1902.11194](https://arxiv.org/abs/1902.11194) [hep-th].
- [11] T. G. Mertens, Towards Black Hole Evaporation in Jackiw-Teitelboim Gravity, *JHEP* **07**, 097, [arXiv:1903.10485](https://arxiv.org/abs/1903.10485) [hep-th].
- [12] T. G. Mertens and G. J. Turiaci, Defects in Jackiw-Teitelboim Quantum Gravity, *JHEP* **08**, 127, [arXiv:1904.05228](https://arxiv.org/abs/1904.05228) [hep-th].
- [13] L. V. Iliesiu and G. J. Turiaci, The statistical mechanics of near-extremal black holes, *Journal of High Energy Physics* **2021**, [10.1007/jhep05\(2021\)145](https://arxiv.org/abs/10.1007/jhep05(2021)145) (2021).
- [14] L. V. Iliesiu, *On 2d gauge theories in jackiw-teitelboim gravity* (2019), [arXiv:1909.05253](https://arxiv.org/abs/1909.05253) [hep-th].
- [15] A. R. Brown, L. V. Iliesiu, G. Penington, and M. Usatyuk, *The evaporation of charged black holes* (2024), [arXiv:2411.03447](https://arxiv.org/abs/2411.03447) [hep-th].
- [16] S. Maulik, X. Meng, and L. A. Pando Zayas, Quantum-corrected hawking radiation from near-extremal kerr-newman black holes, [arXiv:2501.08252](https://arxiv.org/abs/2501.08252) [hep-th].
- [17] G. Lin, L. V. Iliesiu, and M. Usatyuk, The evaporation of black holes in supergravity, [arXiv:2504.21077](https://arxiv.org/abs/2504.21077) [hep-th].
- [18] J. Maldacena, The large-n limit of superconformal field theories and supergravity, *International Journal of Theoretical Physics* **38**, 1113–1133 (1999).
- [19] E. Witten, *Anti de sitter space and holography* (1998), [arXiv:hep-th/9802150](https://arxiv.org/abs/hep-th/9802150) [hep-th].
- [20] J. Maldacena, Non-gaussian features of primordial fluctuations in single field inflationary models, *Journal of High Energy Physics* **2003**, 013–013 (2003).
- [21] J. Schwinger, On the green's functions of quantized fields. i, *Proceedings of the National Academy of Sciences* **37**, 452 (1951), <https://www.pnas.org/doi/pdf/10.1073/pnas.37.7.452>.
- [22] F. J. Dyson, The *s* matrix in quantum electrodynamics, *Phys. Rev.* **75**, 1736 (1949).
- [23] P. Ehrenfest, Bemerkung über die angenäherte Gültigkeit der klassischen Mechanik innerhalb der Quantenmechanik, *Zeitschrift für Physik* **45**, 455 (1927).
- [24] S. Iyer and C. M. Will, Black-hole normal modes: A wkb approach. i. foundations and application of a higher-order wkb analysis of potential-barrier scattering, *Phys. Rev. D* **35**, 3621 (1987).
- [25] E. W. Leaver, An Analytic representation for the quasi normal modes of Kerr black holes, *Proc. Roy. Soc. Lond. A* **402**, 285 (1985).
- [26] E. Berti, V. Cardoso, J. A. González, and U. Sperhake, Mining information from binary black hole mergers: A comparison of estimation methods for complex exponentials in noise, *Physical Review D* **75**, [10.1103/physrevd.75.124017](https://arxiv.org/abs/10.1103/physrevd.75.124017) (2007).
- [27] A. Jansen, Overdamped modes in Schwarzschild-de Sitter and a Mathematica package for the numerical computation of quasinormal modes, *Eur. Phys. J. Plus* **132**, 546 (2017), [arXiv:1709.09178](https://arxiv.org/abs/1709.09178) [gr-qc].
- [28] S. Iyer, Black-hole normal modes: A wkb approach. ii. schwarzschild black holes, *Phys. Rev. D* **35**, 3632 (1987).
- [29] R. A. Konoplya, A. Zhidenko, and A. F. Zinhailo, Higher order wkb formula for quasinormal modes and grey-body factors: recipes for quick and accurate calculations, *Classical and Quantum Gravity* **36**, 155002 (2019).
- [30] C. Gundlach, R. H. Price, and J. Pullin, Late-time behavior of stellar collapse and explosions. i. linearized perturbations, *Physical Review D* **49**, 883–889 (1994).